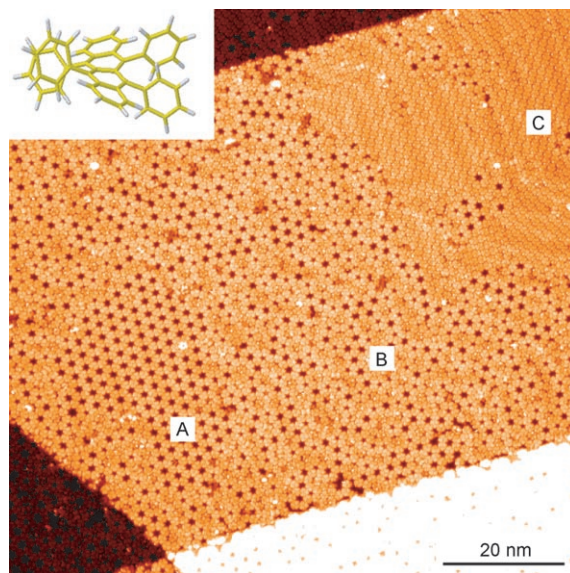


# Two-Dimensional Tiling by Rubrene Molecules Self-Assembled in Supramolecular Pentagons, Hexagons, and Heptagons on a Au(111) Surface\*\*

Marina Pivetta,\* Marie-Christine Blüm, François Patthey, and Wolf-Dieter Schneider

Surface nanostructuring by molecular self-organization is a relevant process in the growing field of nanotechnology. Depending on the characteristics of the molecules and on the type of interactions among them and with the substrate, a variety of surface patterns have been observed by means of scanning tunneling microscopy (STM).<sup>[1]</sup> Indeed, two-dimensional (2D) tiling constitutes a fundamental issue in topology,<sup>[2]</sup> with fascinating examples in nature and art, and applications in many domains such as cellular biology,<sup>[3]</sup> foam physics,<sup>[4]</sup> and crystal growth.<sup>[5]</sup> Herein we present the first observation of surface tiling with both nonperiodic and periodic arrangements of slightly distorted pentagons, hexagons, and heptagons formed by rubrene molecules adsorbed on a Au(111) surface. On adjacent regions of the sample, ordered honeycomb and hexagonal close-packed patterns are found. The existence of manifold arrangements in the supramolecular self-assembly of rubrene on gold originates from the three-dimensional nonplanar flexible structure of the molecule, as well as from the nature of the intermolecular bonds.

Rubrene (5,6,11,12-tetraphenylnaphthacene,  $C_{42}H_{28}$ ) is a nonplanar chiral aromatic hydrocarbon constituted of a twisted tetracene backbone flanked by four out-of-plane phenyl groups as shown in the inset of Figure 1. The survey STM image (Figure 1) shows a Au(111) surface covered by a single layer of rubrene molecules. Three terraces separated by monatomic steps are visible, as well as the Au(111) herringbone reconstruction underlying the molecular layer. This overview shows areas with variable packing densities and different degrees of supramolecular order, denoted by A, B, and C. Regions A and C appear as ordered arrangements: the porous domain A reveals a honeycomb pattern, while region C displays a hexagonal close-packed structure. In contrast, the inhomogeneous area B presents no translational symmetry.



**Figure 1.** STM image of rubrene self-assembled on a Au(111) surface. Domains with different densities and degrees of order, denoted A, B, and C, are visible. Inset: twisted 3D conformation of rubrene.

A detail of the latter nonperiodic phase is shown in Figure 2a. The dashed blue circle surrounds a single rubrene molecule; the submolecular contrast reveals three lobes and a quite regular threefold symmetry.<sup>[6]</sup> The self-assembled pattern is composed of supramolecular pentagons, hexagons, and filled heptagons, which appear to be randomly distributed over the surface. There exist 11 distinct tilings by regular polygons;<sup>[2]</sup> however, a combination of regular pentagons, hexagons, and heptagons generates empty gaps and overlapping regions, as inferred from the consideration of the angles at the corners of a regular pentagon ( $108^\circ$ ), hexagon ( $120^\circ$ ), and heptagon ( $\approx 129^\circ$ ). Only when three hexagons joined and share a common corner is the angular sum exactly  $360^\circ$ . Nevertheless, three configurations exist that yield an angular sum close to  $360^\circ$  (Figure 2b): pentagon-hexagon-heptagon ( $\approx 357^\circ$ ), pentagon-heptagon-heptagon ( $\approx 366^\circ$ ), and hexagon-hexagon-heptagon ( $\approx 369^\circ$ ). The introduction of a slight distortion of the polygons allows a plane-filling tessellation. These three configurations are the most frequently realized in the nonperiodic supramolecular tiling shown in Figure 2a. An example of each combination is superimposed on the STM image. The angular sum of the polygons involved in the patterning is either smaller or larger than the required  $360^\circ$  for a true plane-filling, resulting in

[\*] Dr. M. Pivetta, Dr. M.-C. Blüm, Dr. F. Patthey,  
Prof. Dr. W.-D. Schneider  
Ecole Polytechnique Fédérale de Lausanne (EPFL)  
Institut de Physique des Nanostructures  
1015 Lausanne (Switzerland)  
Fax: (+41) 21-693-0422  
E-mail: marina.pivetta@epfl.ch

Dr. M.-C. Blüm  
Center for NanoScience (CeNS)  
Ludwig-Maximilians-Universität München  
80539 Munich (Germany)

[\*\*] Financial support from the Swiss National Science Foundation is acknowledged.

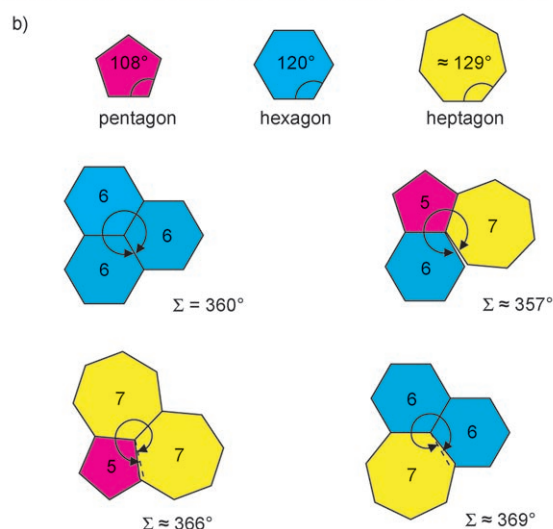
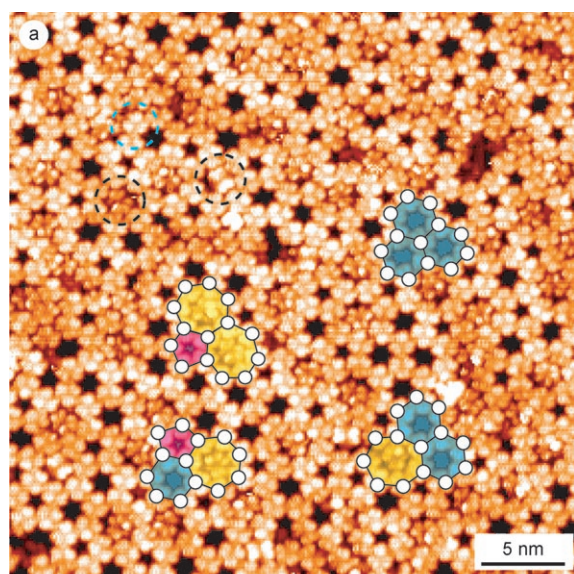


**Figure 2.** a) STM image showing an enlarged view of tiling of type B formed by a nonperiodic assembly of pentagons, hexagons, and filled heptagons. b) Schematic representation of the combinations of pentagons, hexagons, and heptagons resulting in three configurations close to the case of an ideal honeycomb arrangement.

small distortions of the side lengths and the angles of the objects with respect to the geometry of the regular polygons. The STM image in Figure 2a also reveals that the supramolecular heptagons accommodate an additional molecule in their center. These captured specimens present two different appearances, highlighted in Figure 2a by the two dashed black circles. The two conformations presumably arise from the varying small deformations of the heptagons, which offer more circular or more elliptical holes for the additional inserted molecules.

An arrangement of pentagons, hexagons and heptagons that is periodic throughout a whole domain is realized in another type of supramolecular phase present in this mixed molecular layer. An STM image of this tiling (Figure 3) shows a regular arrangement of holes and bright features in the supramolecular pattern. Among these structures, it is possible

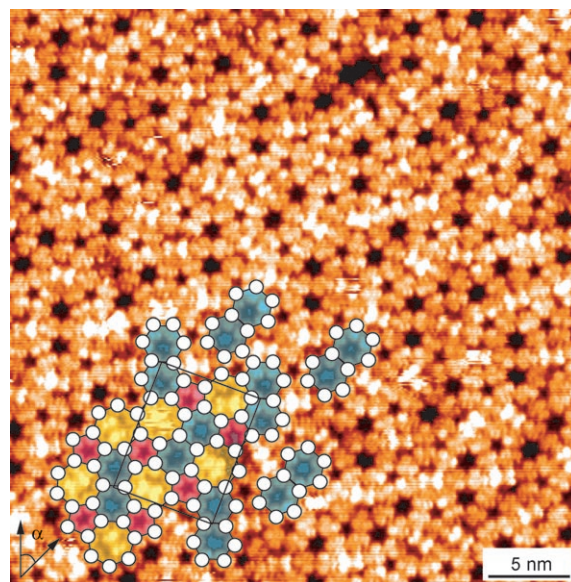


**Figure 3.** STM image revealing a 2D periodic tiling by pentagons, hexagons, and filled heptagons. A possible unit cell is indicated by the rectangle.

to identify pairs of hexagons disposed with regularly alternating angular orientations. These repeating features inclined by an angle  $\alpha \approx 39^\circ$  with respect to each other form a centered rectangular two-dimensional lattice of symmetry  $p2gg$ .<sup>[7]</sup> A possible unit cell is indicated by the rectangle in Figure 3. Four heptagons and four pentagons surrounding each hexagon pair complete this periodic tessellation, as shown in the schematic representation in Figure 3, superimposed on the STM image. This tiling of the surface with slightly distorted pentagons, hexagons, and heptagons uses the above-mentioned configurations of the polygons, which result in the smallest angular deviation from the ideal  $360^\circ$  (i.e. pentagon-hexagon-heptagon, pentagon-heptagon-heptagon, and hexagon-hexagon-heptagon, see Figure 2b) already discussed for the nonperiodic tiling. In this periodic tiling the pentagons and heptagons are always present in pairs, with each pair ideally replacing two hexagons. The replacement of two hexagons with a pentagon-heptagon pair is one of the most common topological defects found in honeycomb structures, such as in graphite and in carbon nanotubes.<sup>[8]</sup> The replacement of all hexagons would generate the so-called pentaheptite structure, a tiling observed in crystallography.<sup>[9]</sup> In the periodic tessellation formed by rubrene, the same number of pentagons, hexagons, and heptagons is present in each unit cell. The molecular density of  $0.50\text{--}0.55\text{ molecules nm}^{-2}$  is close to that of the honeycomb structure. In practice, the density is increased to about  $0.65\text{ molecules nm}^{-2}$  by the systematic presence of the additional molecules inserted into the heptagons. In this periodic tiling the heptagons form a porous template network in which additional host molecules can be accommodated.<sup>[10]</sup>

Another type of ordered, periodic arrangement is the honeycomb phase of area A in Figure 1. Such domains are found next to the nonperiodic tiling discussed above and can extend over hundreds of nanometers. The intermolecular



distance is  $1.2 \pm 0.1$  nm, yielding a packing density of  $0.53 \text{ molecules nm}^{-2}$ . A beautiful singularity existing inside these perfectly periodic domains is shown in the STM image of Figure 4a. The honeycomb pattern is locally interrupted by

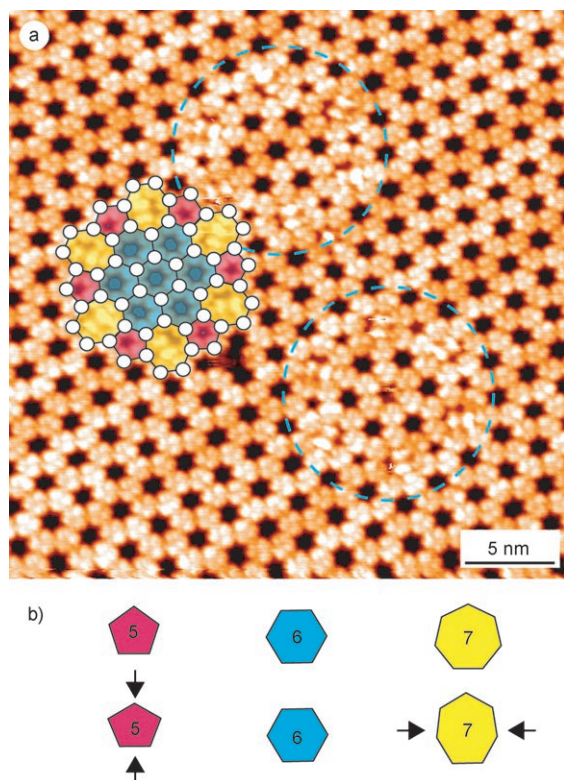


**Figure 4.** a) STM image showing three supramolecular rosettes embedded in a well-ordered honeycomb domain. The schematic drawing of the pattern is superimposed on one of the three rosettes. b) Schematic representation of the distortion of the pentagons and heptagons to compose the tiling.

a circular replacement of twelve hexagons by a ring of six pentagon-heptagon pairs, surrounding a core of seven hexagons. These rosettes are preferentially formed at elbow sites of the herringbone reconstruction of the substrate. In this image three such rosettes are present and dashed blue circles highlight two of them. A schematic representation of the rosette structure superimposed on the third pattern reveals that this symmetric structure with six outer pentagons and six heptagons forms a regular hexagon, which is perfectly insertable into the surrounding honeycomb arrangement. However, the ring of pentagons and heptagons suffer from the constriction from two sides owing to the presence of an inner ring as well as an outer ring of hexagons. Moreover, on the outer side of the rosette the combination pentagon-hexagon-hexagon is present which—with a nominal angular sum of  $348^\circ$ —induces a more important deformation of the pentagons. This angular stress leads to a compression of both the pentagons and the heptagons in opposite directions, as illustrated in Figure 4b. Again, within the supramolecular rosettes the heptagons are filled with additional molecules, exhibiting mainly the elongated conformation.

In the submonolayer regime, the self-assembly of rubrene on Au(111) results in a variety of distinct phases. As a function of the molecular coverage, honeycomb islets, supramolecular pentagonal chains, and close-packed islands have been observed.<sup>[6]</sup> The periodic and nonperiodic tilings presented here demonstrate in an especially fancy manner the conformational flexibility of the rubrene molecules. Supramolecular self-assembly results from the contributions of molecule–substrate and molecule–molecule interactions. Intermolecular bonds are mainly based on weak, noncovalent interactions such as dipole–dipole (or higher order multipole) forces, hydrogen bonds, or van der Waals (vdW) interactions.<sup>[1,11]</sup> Given the absence of a dipole moment, the bonding between rubrene molecules might have contributions from electrostatic quadrupole–quadrupole interactions, vdW forces, and  $\pi \cdots \pi$  and  $\text{CH} \cdots \pi$  bonding. Among them, vdW forces are isotropic, the other interactions are directional. While the  $\pi \cdots \pi$  interaction favors a parallel arrangement of the  $\pi$  systems,<sup>[12]</sup> the  $\text{CH} \cdots \pi$  bond is particularly strong for a CH group oriented perpendicular to a  $\pi$  system of another molecule.<sup>[13]</sup> These forces relying on the existence of  $\pi$  systems are effectively realized between rubrene molecules owing to the nonplanar aromatic tetracene backbone, the four phenyl groups, and the presence of 28 CH bonds pointing into three dimensions (inset in Figure 1). The directional interactions can account for the formation of the ordered hexagonal structures, in which the bond angle between molecules is precisely  $120^\circ$ . Intriguingly, a small modification of the intermolecular bonds or a slight change in the molecular conformation results in the formation of pentagons and heptagons. The adaptive behavior of rubrene allows these modifications and leads to the observed 2D periodic and nonperiodic tilings with pentagons, hexagons, and heptagons.

## Experimental Section

The experiments were carried out with a home-built scanning tunneling microscope (STM) operated in ultrahigh vacuum at a temperature of 50 K. The rubrene molecules were thermally evaporated on a well-prepared Au(111) surface held at room temperature. All the STM images presented here were acquired in constant current mode, with typical tunneling parameters:  $V_{\text{bias}} = -0.8$  V,  $I = 100$  pA.

Received: September 28, 2007

Published online: December 28, 2007

**Keywords:** rubrene · scanning probe microscopy · self-assembly · supramolecular chemistry

- [1] a) S. De Feyter, F. C. De Schryver, *Chem. Soc. Rev.* **2003**, 32, 139; b) J. V. Barth, *Annu. Rev. Phys. Chem.* **2007**, 58, 375.
- [2] B. Grünbaum, G. C. Shephard, *Tilings and Patterns*, Freeman, New York, **1987**.
- [3] a) J. Stavans, *Rep. Prog. Phys.* **1993**, 56, 733; b) B. Dubertret, T. Aste, H. M. Ohlenbusch, N. Rivier, *Phys. Rev. E* **1998**, 58, 6368.
- [4] F. Graner, Y. Jiang, E. Janiaud, C. Flament, *Phys. Rev. E* **2000**, 63, 011402.
- [5] G. Ungarn, X. Zeng, *Soft Matter* **2005**, 1, 95.
- [6] a) M.-C. Blüm, E. Čavar, M. Pivetta, F. Patthey, W.-D. Schneider, *Angew. Chem.* **2005**, 117, 5468; *Angew. Chem. Int. Ed.* **2005**, 44,

- 5334; b) M.-C. Blüm, M. Pivetta, F. Patthey, W.-D. Schneider, *Phys. Rev. B* **2006**, 73, 195409.
- [7] K. E. Plass, A. L. Grzesiak, A. J. Matzger, *Acc. Chem. Res.* **2007**, 40, 287.
- [8] a) A. J. Stone, D. J. Wales, *Chem. Phys. Lett.* **1986**, 128, 501; b) P. Simonis, C. Goffaux, P. A. Thiry, L. P. Biro, P. Lambin, V. Meunier, *Surf. Sci.* **2002**, 511, 319; c) A. Hashimoto, K. Suenaga, A. Gloter, K. Urita, S. Iijima, *Nature* **2004**, 430, 870.
- [9] a) V. H. Crespi, L. X. Benedict, M. L. Cohen, S. G. Louie, *Phys. Rev. B* **1996**, 53, R13303; b) M. Deza, P. W. Fowler, M. Shtogrin, K. Vietze, *J. Chem. Inf. Comput. Sci.* **2000**, 40, 1325.
- [10] a) J. A. Theobald, N. S. Oxtoby, M. A. Phillips, N. R. Champness, P. H. Beton, *Nature* **2003**, 424, 1029; b) M. Stöhr, M. Wahl, H. Spillmann, L. H. Gade, T. A. Jung, *Small* **2007**, 3, 1336.
- [11] G. R. Desiraju, *Nature* **2001**, 412, 397.
- [12] a) C. A. Hunter, J. K. M. Sanders, *J. Am. Chem. Soc.* **1990**, 112, 5525; b) C. A. Hunter, K. R. Lawson, J. Perkins, C. J. Urch, *J. Chem. Soc. Perkin Trans. 2* **2001**, 651.
- [13] a) M. Tamres, *J. Am. Chem. Soc.* **1952**, 74, 3375; b) M. Nishio, M. Hirota, Y. Umezawa, *The CH/ $\pi$  Interaction: Evidence, Nature, and Consequences*, Wiley, New York, **1998**; c) U. Samanta, P. Chakrabarti, J. Chandrasekhar, *J. Phys. Chem. A* **1998**, 102, 8964; d) S. Tsuzuki, K. Honda, T. Uchimaru, M. Mikami, K. Tanabe, *J. Am. Chem. Soc.* **2000**, 122, 3746; e) M. Nishio, *Cryst. Eng. Commun.* **2004**, 6, 130.